Supporting Information

Short lipid-conjugated pH sensors for imaging of transporter activities in reconstituted systems and living cells

Ronja Marie Kühnel[†a], Marta Grifell Junyent[†ab], Ida Louise Jørgensen[ab], Gerdi Christine Kemmer[#b], Jürgen Schiller[c], Michael G. Palmgren,[b] Bo Højen Justesen[*a], Thomas Günther Pomorski[*ab]

[a]Faculty of Chemistry and Biochemistry, Department of Molecular Biochemistry, Ruhr University Bochum, Universitätstrasse 150, D-44780 Bochum, Germany

[b]Department of Plant and Environmental Sciences, University of Copenhagen, Thorvaldsensvej 40, 1871 Frederiksberg C, Denmark

[c]Institute of Medical Physics and Biophysics, Faculty of Medicine, University of Leipzig, 04107 Leipzig, Germany

[†]These authors contributed equally to the work.

[#]Current address: Kinvest GmbH, Südliche Münchner Str. 32, 82031 Grünwald, Germany

List of contents

1. TLC analysis of DOPE-conjugated pHrodo green and red after synthesis using reaction conditions R1-R4.

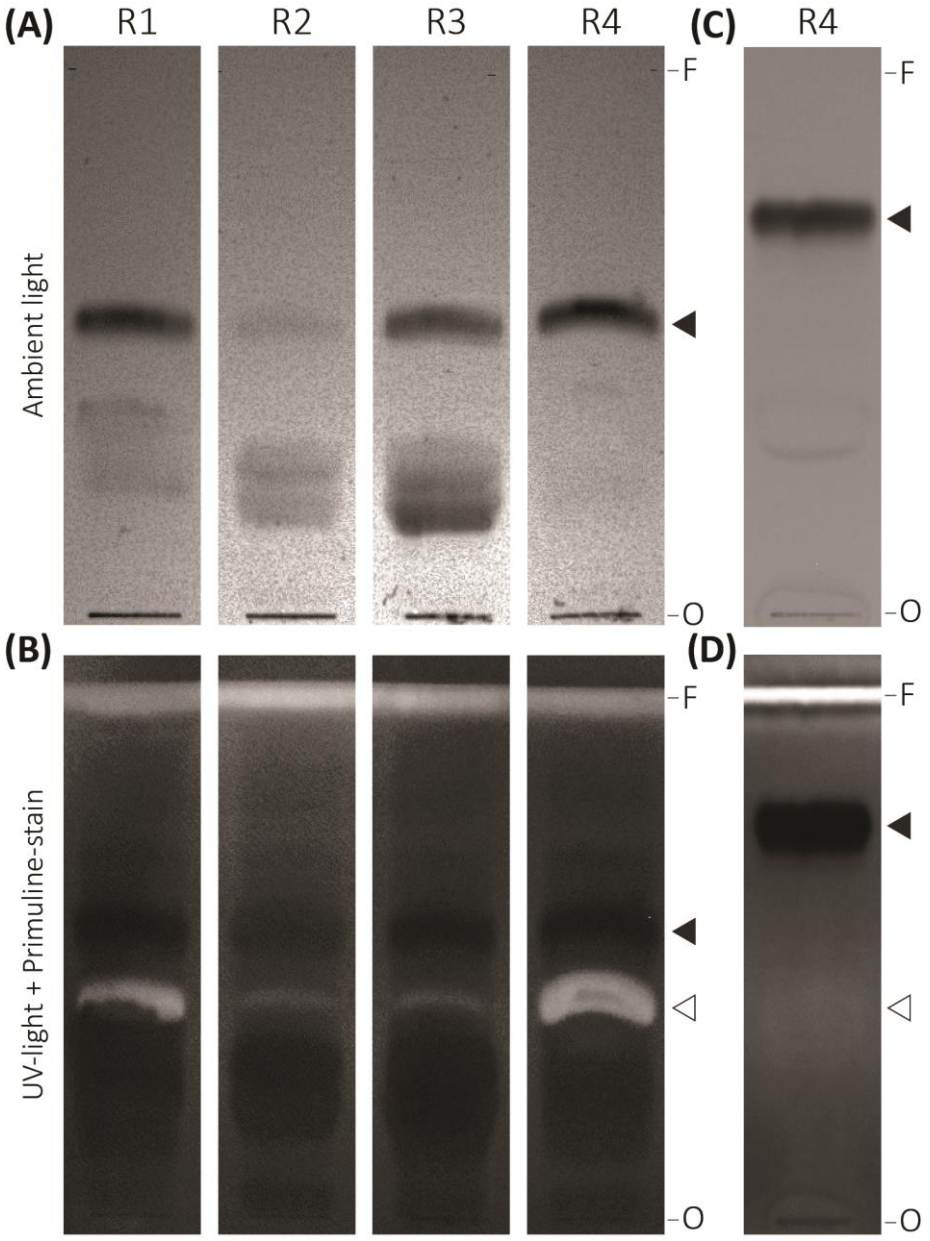

Fig. S1 TLC analysis of DOPE-conjugated pHrodo Green (A, B) and pHrodo Red (C, D) after synthesis under four different reaction conditions (R1-R4) as specified in Table 1. Products were separated by alkaline TLC, silica plates were dried completely before imaging under ambient light (A, C) and under UV-light after staining with primuline (B, D). Filled arrowheads indicate the lipid-conjugated fluorophore, open arrowhead unreacted DOPE. Product bands were extracted and identified via MALDI-TOF mass spectrometry. Analysis under ambient light revealed for all conditions a common product band with Rf value of 0.55 for DOPE-pHrodo™ Green. Unreacted DOPE appeared after primuline-staining under UV-light with Rf value of 0.40. While reactions R1-R3 resulted in by-product formation, as assessed by several additional bands detectable under ambient and UV light, reaction R4 led to efficient product formation with essentially no by-product formation and a yield of about 90%. Likewise, coupling of the amine-reactive succinimidyl ester of pHrodo™ Red to DOPE resulted in yields of about 90% without appreciable by-product formation when performed under condition R4. O: origin, F: solvent front.

2. Analytical characterization of the lipid-conjugated sensors by mass spectrometry

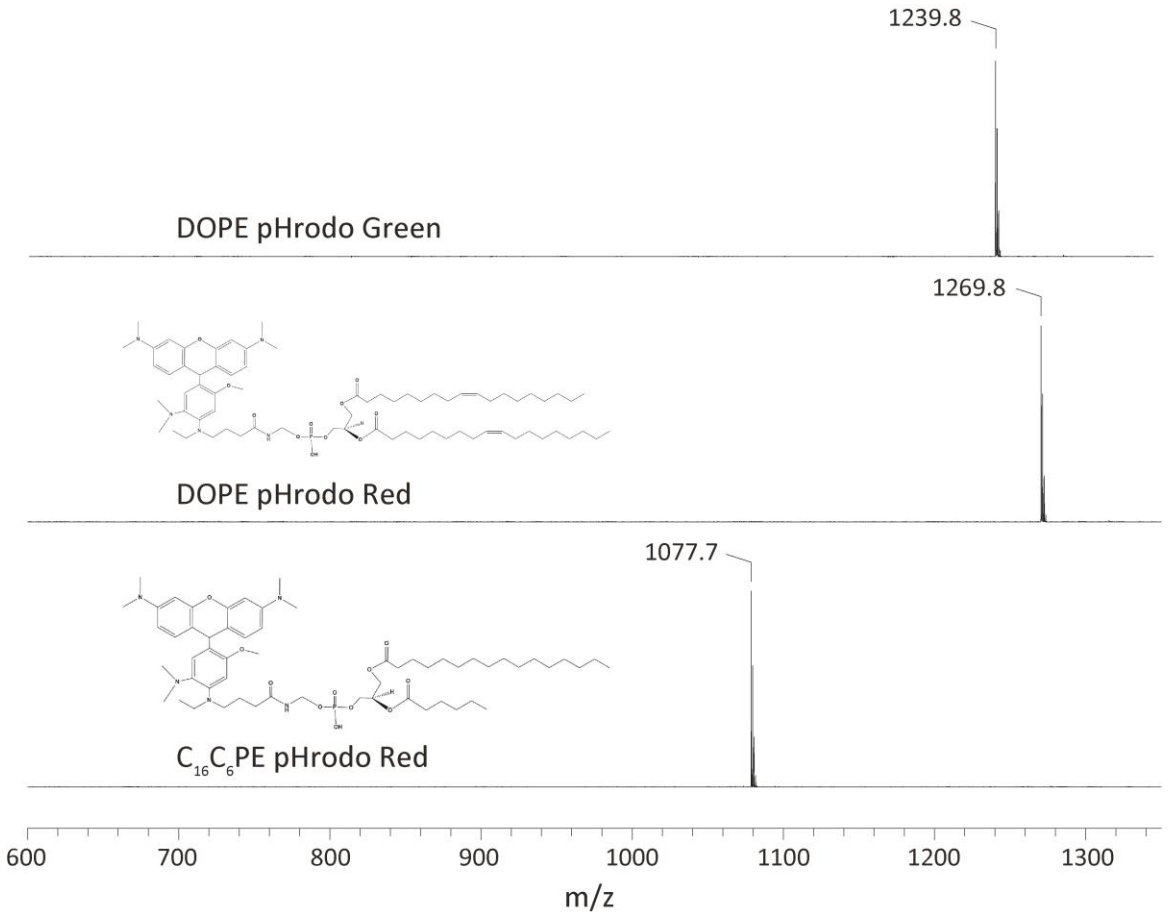

Fig. S2 Analytical characterization of the lipid-conjugated sensors by mass spectrometry. Negative ion MALDI-TOF mass spectra were acquired on a Bruker Autoflex MALDI-TOF mass spectrometer in the reflector mode. 9-aminoacridine (9-AA) in isopropanol/acetonitrile served as the matrix in all cases. Peaks are marked by the *m/z* ratios and the assignments of the different compounds are given directly at the respective traces. Note the complete lack of any starting material. *Inset*: chemical structure of pHrodo-DOPE; chemical structure of pHrodo Red is based on M. Ogawa, N. Kosaka, C. A. Regino, M. Mitsunaga, P. L. Choyke and H. Kobayashi, Mol. BioSyst., 2010, 6, 888–893.

3. pH-Sensitivity of short-chain lipid-conjugated fluorescent pH indicators

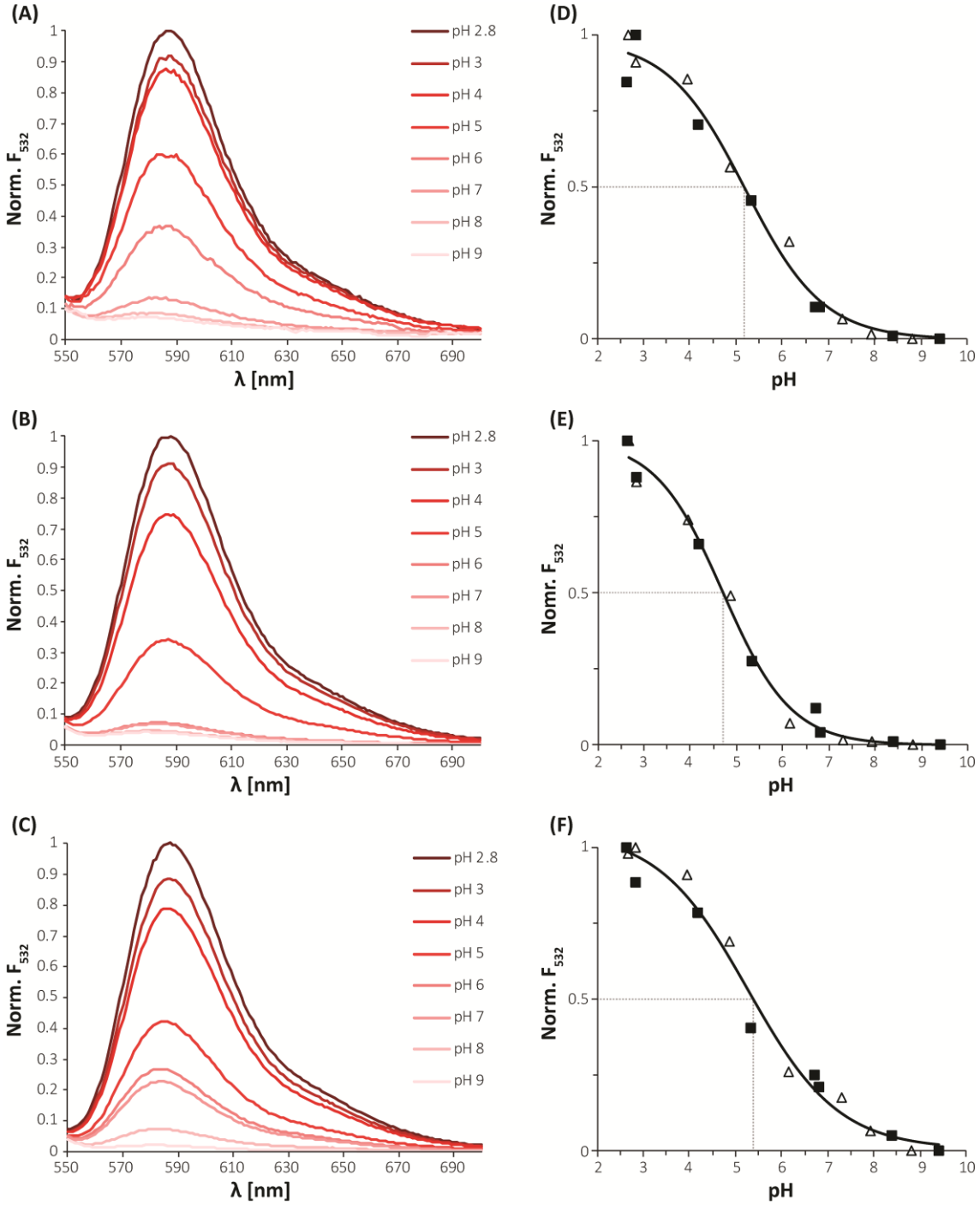

Fig. S3 pH-dependent fluorescence properties of short-chain lipid-conjugated fluorescent pH indicators. Fluorescence emission spectra of vesicle-embedded diC_6- (A), diC_8- (B) and $C_{16}C_6$-PE (C) pHrodo Red in buffer solutions of different pH values upon excitation at 532 nm. All measurements were performed in pH-adjusted buffers of the indicated pH values containing the protonophore CCCP (5 µM) and the K^+-ionophore valinomycin (62.5 nM) to equilibrate the pH between the inside and outside of the liposomes. Each spectrum represents an aliquot of a liposome stock solution diluted in buffer and incubated for at least 15 min. pH-titration curves of vesicle-embedded diC_6- (D), diC_8- (E) and $C_{16}C_6$-PE (F) pHrodo Red. Different symbols denote independent experiments (n=2); lines represent global nonlinear least square fits to the Boltzmann function. Norm. F, max fluorescence intensity for each pH was normalised to the maximum value.

4. Stable inner membrane localization of the lipid-conjugated pH sensors

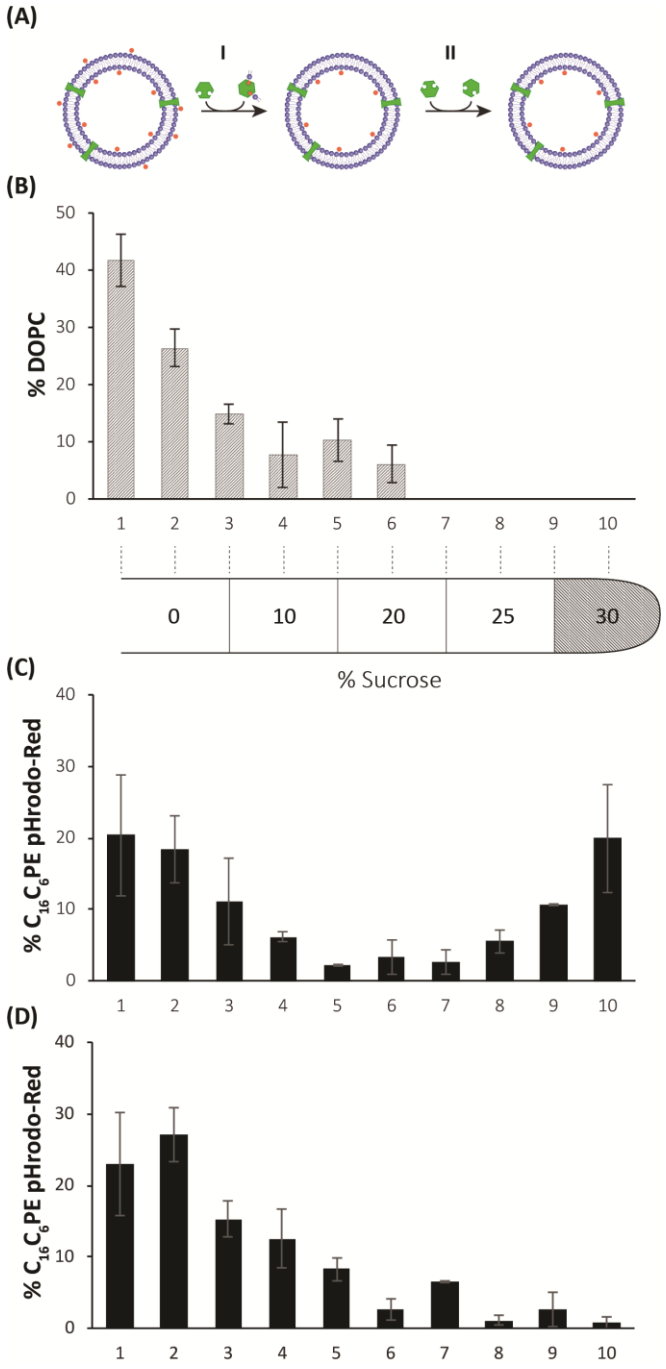

Fig. S4 Inner membrane localization of the lipid-conjugated pH sensors in asymmetrically labelled proteoliposomes is stable. Asymmetrically $C_{16}C_6$-PE-pHrodo labelled proteoliposomes with reconstituted plasma membrane H^+-ATPase were prepared by overnight incubation with albumin and isolated by floatation on a sucrose density gradient [25, 20, 10, and 0% (w/w)], (A, I). After pooling and storage of the isolated vesicles (fractions 1-3) for 24 h at 4 °C, stability of the inner membrane localization of the lipid-conjugated pH sensors was tested by a second overnight incubation with albumin followed by floatation on a sucrose density gradient, (A, II). The gradients were centrifuged (280,000 x g, 14 h), and fractions were collected as indicated and analyzed for fluorescence and phospholipid content. (B) Phospholipid content of the gradient fractions showing the flotation of the vesicles to upper gradient steps [0-10% (w/w) sucrose]. (C) pHrodo fluorescence of the gradient fractions after the first back extraction, demonstrating efficiently removal of the short-chain lipid-conjugated pH sensor from the outer vesicle leaflet. (D) pHrodo fluorescence of the gradient fractions after albumin re-extraction of asymmetrically labelled proteoliposomes, demonstrating the exclusive localization of the short-chain lipid-conjugated pH sensor even after overnight storage. Error bars show S.D. from at least two independent experiments.

5. Conversion of fluorescence intensity to pH

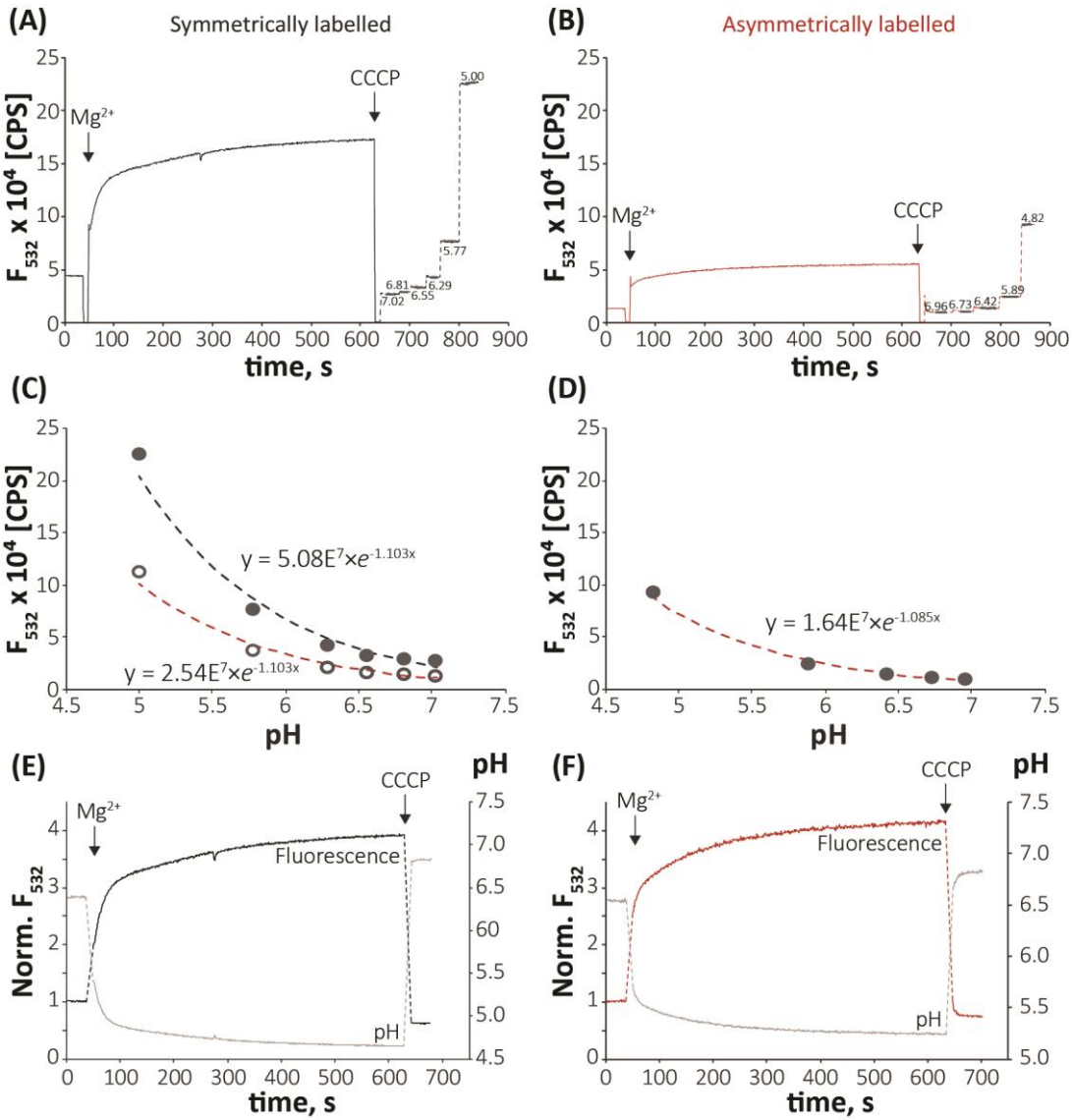

Fig. S5 Conversion of fluorescence intensity into pH. Fluorescence traces of symmetrically (A) and asymmetrically labelled proteoliposomes (B) during proton pumping measurement, followed by addition of the ionophore CCCP and sequential titration of 0.1M HCl (stipled lines) with concurrent measurement of pH as indicated. Fluorescence to pH calibration curves were created for symmetrically (C) and asymmetrically labelled proteoliposomes (D) by plotting the average CPS versus measured pH (bold markings in A, and C). An exponential function was fitted to the data points (stipled lines in C and D). Normalized CPS with corresponding pH traces of symmetrically (E) and asymmetrically labelled proteoliposomes (F) during proton pumping measurement. Due to the presence of pH sensor on both leaflets of the symmetrically labelled proteoliposomes, the conversion of fluorescence into pH was accomplished by substracting the half-background of the initial signal, taken as contribution of the outer located pH sensor, and using a calibration curve of half the fluorescence signal (red curve in C). This is in contrast to asymmetrically labelled proteoliposomes where no background signal was substracted, based on the exclusive location of the pH sensor in the inner leaflet of the proteoliposomes, and where the full pH calibration curve was used (red curve in D).

6. Cell surface staining with $C_{16}C_6$-PE-pHrodo Red

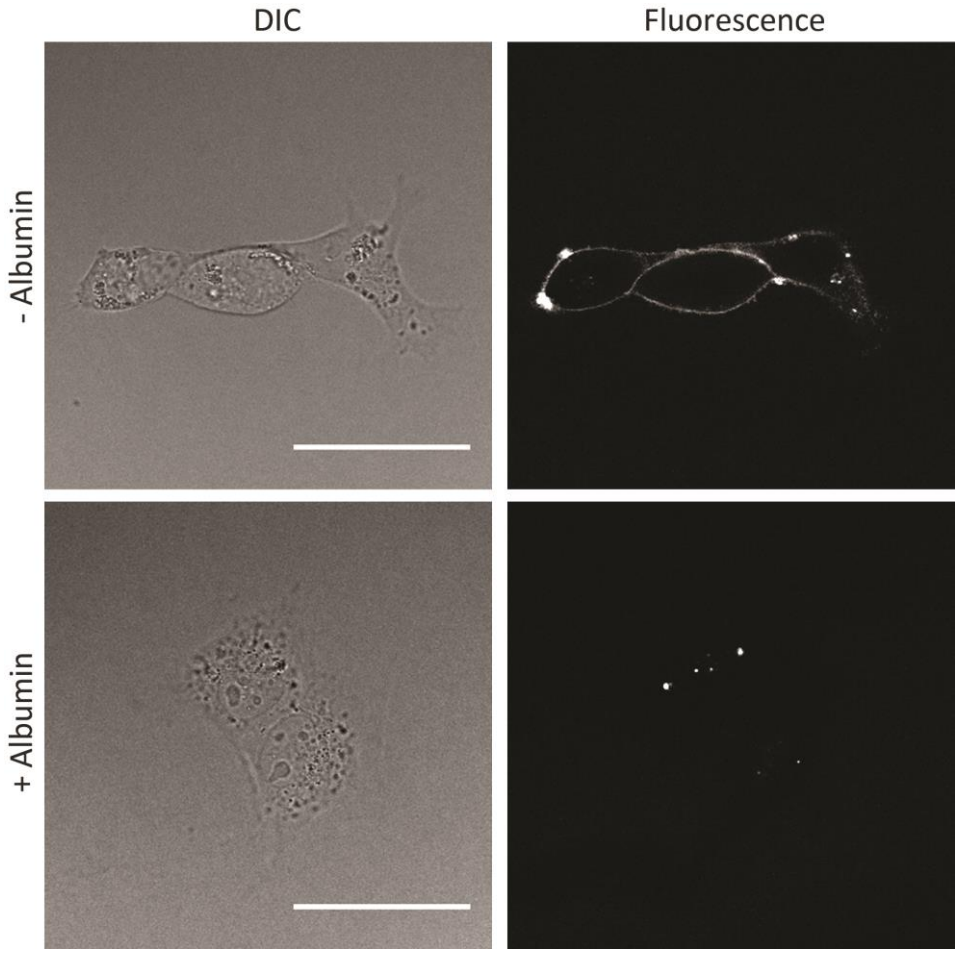

Fig. S6 Cell surface staining with $C_{16}C_6$-PE-pHrodo Red at 2 °C. COS-7 cells were imaged after labelling for 30 min at 2 °C (-Albumin) and after back-exchange with albumin (+Albumin). Cells were imaged in pH 5.5 medium by differential interference contrast (DIC) and fluorescence microscopy. The fluorescence of $C_{16}C_6$-PE-pHrodo Red was exclusively detected at the plasma membrane under these conditions. Back-exchange to albumin efficiently removed the lipid-linked sensor from the outer leaflet of the plasma membrane. Bars, 50 µm.

7. Fluorescence of $C_{16}C_6$-PE-pHrodo Red labelled cells in response to NH_4Cl

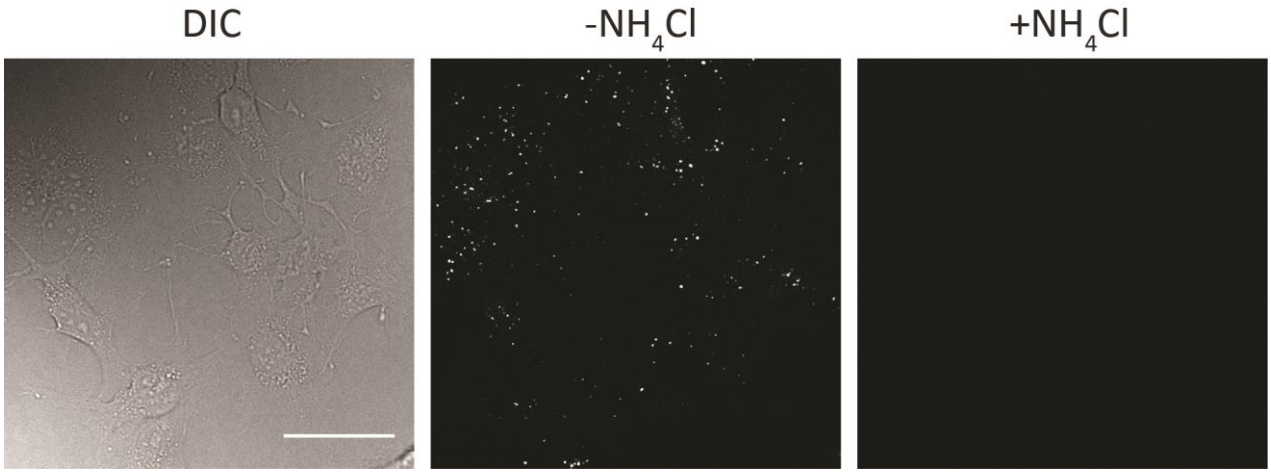

Fig. S7 Fluorescence of $C_{16}C_6$-PE-pHrodo Red labelled cells in response to NH_4Cl. COS-7 cells were labelled with $C_{16}C_6$-PE-pHrodo Red and incubated for 30 min at 37 °C to allow endocytosis. Subsequently, cells were incubated in pH 7.4 medium and exposed to 10 mM NH_4Cl as indicated. Cells were imaged by differential interference contrast (DIC) and fluorescence microscopy. Bars, 50 µm.

8. Effect of prolonged incubation on pHrodo Green dextran and lipid-conjugated pHrodo Red cellular fluorescence

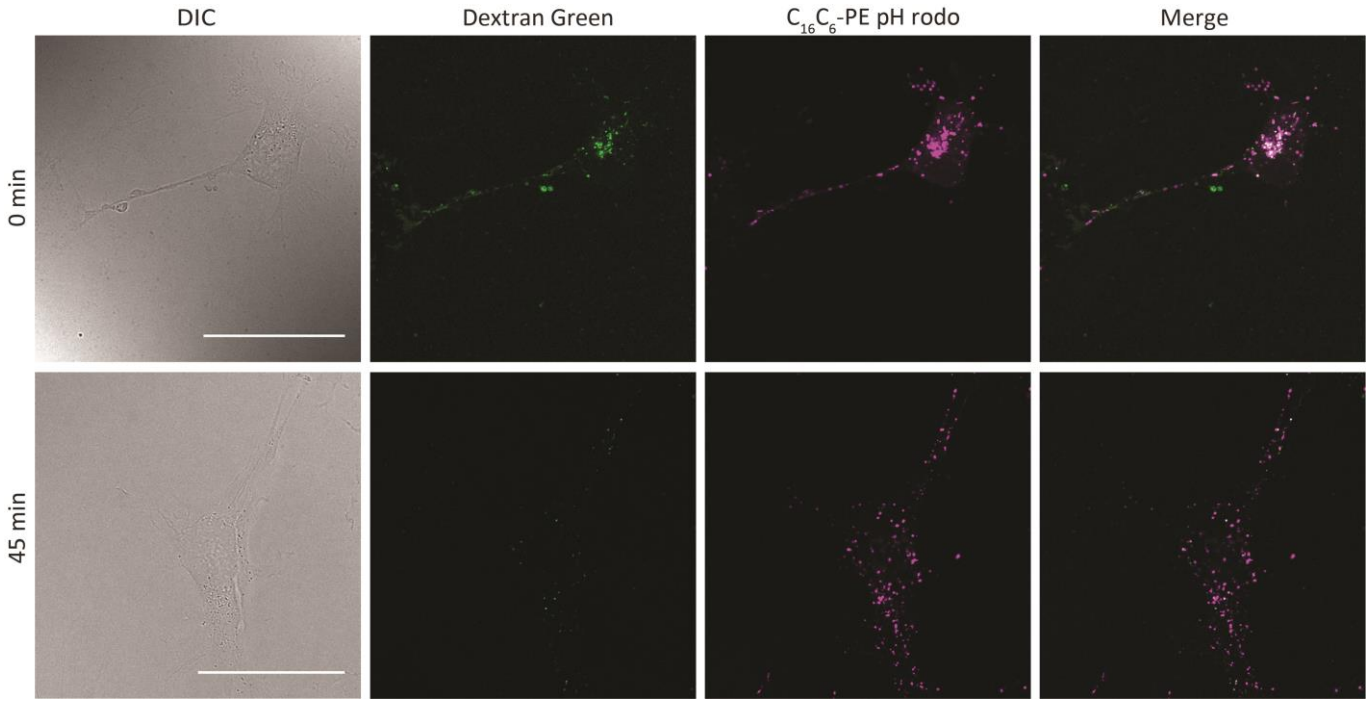

Fig. S8 Effect of prolonged incubation on Green dextran and lipid-conjugated pHrodo Red cellular fluorescence. COS-7 cells labelled with $C_{16}C_6$-PE-pHrodo Red at 2 °C were incubated for 30 min at 37 °C in the presence of the soluble pH marker pHrodo Green dextran. Subsequently, cells were washed and incubated in fluorophore-free pH 7.4 medium supplemented with 10% (wt/v) albumin for 45 min at 37 °C. Cells were imaged after incubation with pHrodo Green dextran (0 min) and after 45 min-incubation in fluorophore-free medium (45 min) by differential interference contrast (DIC) and confocal fluorescent microscopy. In contrast to the labelling by lipid-conjugated pHrodo Red, intracellular staining of pHrodo Green dextran is rapidly lost during incubation in fluorophore-free medium. Bars, 50 µm.

9. pH titration in cells loaded with $C_{16}C_6$-PE-pHrodo Red

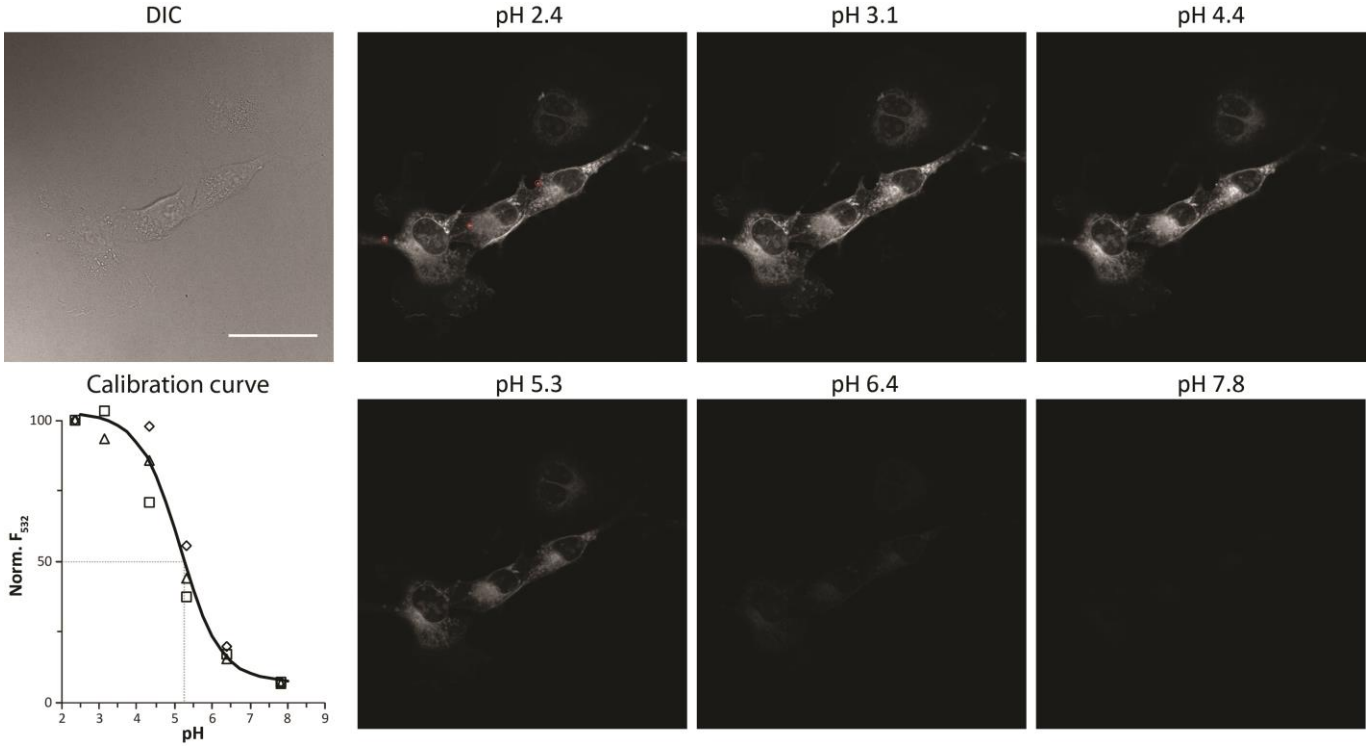

Fig.S9 pH dependent change of fluorescence in $C_{16}C_6$-PE-pHrodo-Red loaded COS-7 cells exposed to the indicated pH values using nigericin/valinomycin and high K^+. Cells were imaged after 5 min of incubation in the pH-adjusted buffers of the indicated pH values by differential interference contrast (DIC) and confocal fluorescence microscopy. Bars, 50 µm. A pH calibration curve was created from analysis of three regions of interest using ImageJ (ROIs, red circles in pH 2).

10. Stability and cytotoxicity of $C_{16}C_6$-PE-pHrodo Red

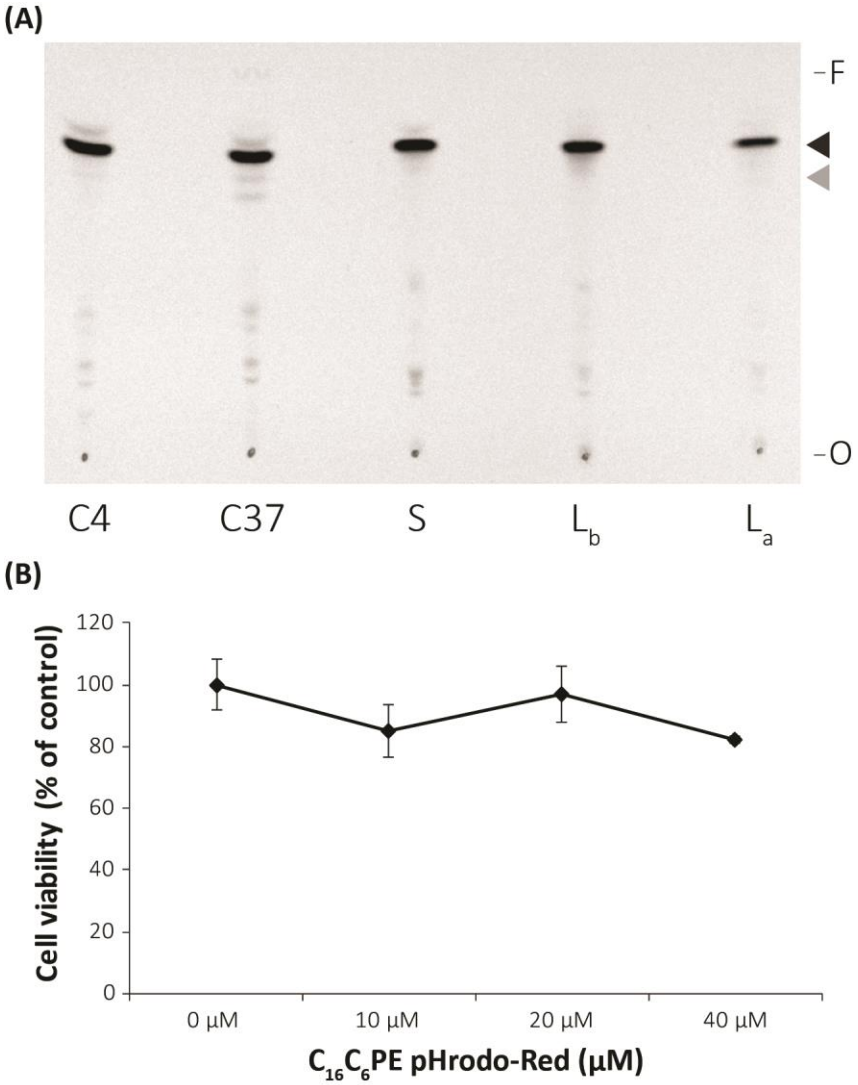

Fig. S10 Stability and cytotoxicity of $C_{16}C_6$-PE-pHrodo Red. (A) COS-7 cells were labelled with $C_{16}C_6$-PE-pHrodo Red at 2 °C for 30 min and then incubated for 30 min at 2 °C and 37 °C. Total lipids were extracted from the cells and the labelling solutions, separated on TLC, and concentrations of non-converted $C_{16}C_6$-PE-pHrodo Red were analysed using a Biorad Chemidoc Imaging System. A representative TLC plate of total lipid extracts prepared from cells incubated at 2 °C and 37 °C (C2 and C37) and the labelleing solutions before (L_b) and after (L_a) labelling are shown. Quantative analysis revealed that breakdown of $C_{16}C_6$-PE-pHrodo Red at 2°C and 37°C was 4.8% and 10%, respectively. $C_{16}C_6$-PE-pHrodo Red standard (S) was chromatographed on the same plate. The positions of $C_{16}C_6$-PE-pHrodo Red and its breakdown product are indicated by a black and gray arrowhead, respectively. O, origin; F, front. (B) Cell viability after incubation with different concentrations of $C_{16}C_6$-PE-pHrodo Red for 60 min at 37 °C, as determined by the MTT assay. Absorbance values were measured at 570 nm and 690 nm using a plate reader (ClarioStar, BMG Labtech). The viability of the cells in the absence of the $C_{16}C_6$-PE-pHrodo Red is defined as 100%.